An ab Initio Study on Thermal Rearrangement Reactions of 1-Silylprop-2-en-1-ol $H_3SiCH(OH)CH{=}CH_2$

Yongming Yu,[†,‡] Shengyu Feng,*[,†] and Dacheng Feng[†]

School of Chemistry and Chemical Engineering, Shandong University, Jinan 250100, P.R. China, and School of Chemistry and Chemical Engineering, Qingdao University, Qingdao 266071, P.R. China

Received: September 11, 2004; In Final Form: February 21, 2005

The thermal rearrangement reactions of 1-silylprop-2-en-1-ol $H_3SiCH(OH)CH{=}CH_2$ were studied by ab initio calculations at the G2(MP2) and G3 levels. The reaction mechanisms were revealed through ab initio molecular orbital theory. On the basis of the MP2(full)/6-31G(d) optimized geometries, harmonic vibrational frequencies of various stationary points were calculated. The reaction paths were investigated and confirmed by intrinsic reaction coordinate (IRC) calculations. The results show that the thermal rearrangements of $H_3SiCH(OH)CH{=}CH_2$ happen in two ways. One is via the Brook rearrangement reactions (reaction A), and the silyl group migrates from carbon atom to oxygen atom passing through a double three-membered ring transition state, forming allyloxysilane $CH_2{=}CHCH_2OSiH_3$. In the other, the reactant undergoes a dyotropic rearrangement; the hydroxyl group migrates from carbon atom to silicon atom coupled with a simultaneous migration of a hydrogen atom from silicon atom to carbon atom, forming allylsilanol $CH_2{=}CHCH_2SiH_2OH$ (reaction B). The barriers for reactions A and B were computed to be 343.5 and 203.7 kJ/mol, respectively, at the G3 level. The changes of the thermodynamic functions, entropy (ΔS), entropy ($\Delta S^{\ddagger}$) for the transition state, enthalpy (ΔH), and free energy (ΔG) were calculated by using the MP2(full)/6-31G(d) optimized geometries, and harmonic vibrational frequencies of reactants, transition states, and products with statistical mechanical methods, and equilibrium constant $K(T)$ and reaction rate constant $k(T)$ in canonical variational transition-state theory (CVT) with centrifugal-dominant small-curvature tunneling approximation (SCT) were calculated over a temperature range 400−1300 K. The conventional transition-state theory (TST) rate constants were also calculated for the purposes of comparison. The influences of the vinyl group attached to the center carbon of the α-silyl alcohols on reactions were discussed.

1. Introduction

Carbofunctional organosilicon compounds play important roles in organosilicon chemistry. For example, they could be used to synthesize new organosilicon compounds or polymers, or to modify organosilicon or organic polymers.[1] However, because of the rearrangement or decomposition under certain conditions, their applications are limited to some extent. Understanding their rearrangement conditions and mechanisms will be of great importance for the control and application of these reactions and compounds.

The [1,2] rearrangement reactions of the silyl group in α-silyl alcohols from carbon to oxygen atoms[2−10] and in alkyloxysilanes from oxygen to carbon atoms[11−13] under either strong base[2,3,11,12] or peroxide initiating conditions[4−10,13] are known as Brook and Wright−West rearrangements, respectively (Scheme 1). Studies on the mechanisms of these reactions have been focused both experimentally[2,3,8−10,13] and theoretically.[14−17] The ab initio investigations of rearrangement reactions of $[H_2COSiH_3]^-$ and $[H_2COSiH_3]Na$ by Tonachini[14,15] and Wang[16] suggest that the Brook or Wright−West rearrangement under the strong base condition occurs via a three-membered-ring intermediate (Scheme 2a) in which silicon is pentacoordinate, whereas Schiesser[17] suggested that the rearrangement of $[H_3SiCH_2O]^{\bullet}$ initiated by peroxides proceeds via a three-membered-ring transition state (Scheme 2b) in which silicon is also pentacoordinate. Up to now, however, no reports on thermal Brook or Wright−West rearrangement have been found. But actually, hydroxyalkyl organosilicon compounds or polymers are often used under high-temperature conditions. Therefore, understanding their thermal stability or rearrangements is of practical value. For this reason, we reported the results of our studies on the thermal rearrangement reactions of silylmethanol.[18] The results show that, different from the rearrangement under strong base conditions, two rearrangement reactions may occur when silylmethanol is heated. One is via the Brook rearrangement reaction, in which the silyl group migrates from carbon to oxygen atom passing through a double three-membered-ring transition state, forming methyloxysilane CH_3OSiH_3; in the other, the reactant undergoes a dyotropic rearrangement, a kind of reaction named by Reetz,[19]

SCHEME 1

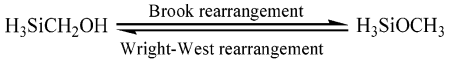

SCHEME 2

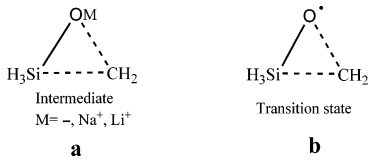

* To whom correspondence should be addressed. E-mail: fsy@sdu.edu.cn. Fax: 86-531-8564464.
† Shandong University.
‡ Qingdao University.

10.1021/jp045892u CCC: $30.25
Published on Web 04/05/2005

SCHEME 3

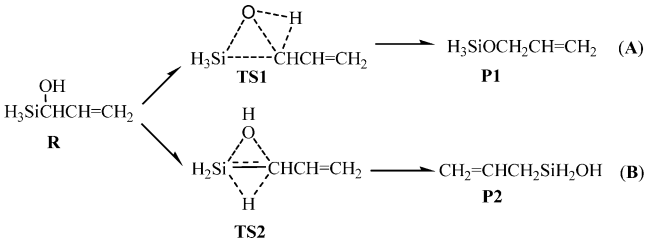

in which the hydroxyl group migrates from carbon to silicon atom coupled with a simultaneous migration of a hydrogen atom from silicon to carbon atom via a double three-membered-ring transition state, forming methylsilanol CH_3SiH_2OH. The dyotropic reaction is preferred to the Brook rearrangement reaction both thermodynamically and kinetically. To investigate the effects of substituents attached to the α-carbon atom on the rearrangement reactions of α-silyl alcohols, we carried out the same calculations on 1-silylprop-2-en-1-ol $H_3SiCH(OH)CH{=}CH_2$. The results will be reported in this paper.

2. Theoretical Methods

Optimized geometries for the stationary points were calculated at the MP2(full)/6-31G(d) levels. The corresponding harmonic vibrational frequencies (scaled by 0.9427[20]) were calculated at the MP2(full)/6-31G(d) levels in order to verify whether the stationary points are local minima or first-order saddle points. Energies of stationary points were obtained at the G2(MP2)[21] and G3[22] levels. The reaction paths were examined by intrinsic reaction coordinate (IRC) calculations at the MP2(full)/6-31G(d) level. All calculations were carried out by using the *Gaussian 98*, revision A.9 series of programs.[23] The changes of thermodynamic functions, entropy (ΔS), entropy ($\Delta S^{\ddagger}$) for the transition state, enthalpy (ΔH), and free energy (ΔG) of reactions were calculated by using the MP2(full)/6-31G(d) optimized geometries and harmonic vibrational frequencies of reactants, transition states, and products with statistical mechanical methods.[24] The rate constants ($k(T)$) of the reactions were calculated by using the canonical variational transition-state theory (CVT).[25−27] Torsional modes of transition states were identified by direct inspection of low-frequency modes and treated as hindered internal rotations using the method of hindered rotor approximation with the RO scheme and the SC level.[28] The tunneling effect was considered and calculated using the centrifugal-dominant small-curvature tunneling approximation (SCT).[29] All of the kinetic calculations were carried out using the *POLYRATE 9.0* program.[30]

3. Results and Discussion

Consistent with the results of the previous studies[18] on silylmethanol, the thermal rearrangements of $H_3SiCH(OH)CH{=}CH_2$ (**R**) could happen in two ways (see Scheme 3). One is Brook rearrangement, in which the silyl group of **R** migrates from carbon atom to oxygen atom passing through the double three-membered-ring transition state **TS1**, as shown in path A of Scheme 3, forming allyloxysilane **P1**; the other is a dyotropic rearrangement, in which the hydroxyl group of **R** migrates from carbon atom to silicon atom coupled with a simultaneous migration of a hydrogen atom from silicon atom to carbon atom via transition state **TS2**, as shown in path B of Scheme 3, forming allylsilanol **P2**. The two pathways of the reactions were investigated.

3.1. Stationary Points. Geometries of $H_3SiCH(OH)CH{=}CH_2$ and its rearrangement products and transition states are given in Figure 1, and the corresponding structural parameters and energies (via zero-point energy, or ZPE, corrections) are listed in Tables 1 and 2, respectively.

Stable conformations of reactant **R** and products **P1** and **P2** (3 for **R**, 3 for **P1**, and 9 for **P2**) were located. For the purpose of this paper, only the most stable conformations of each species (**R1a**, **P1b**, and **P2b**) and those corresponding to transition states (**P1a** and **P2a**) are listed in Figure 1.

The calculations show that the energy differences between **P1a** and **P1b** and **P2a** and **P2b** are only 0.8 and 4.1 kJ/mol, respectively, at the G3 level. In **P1,** the groups on the carbon and silicon atoms are inter-overlapped. Other geometries in

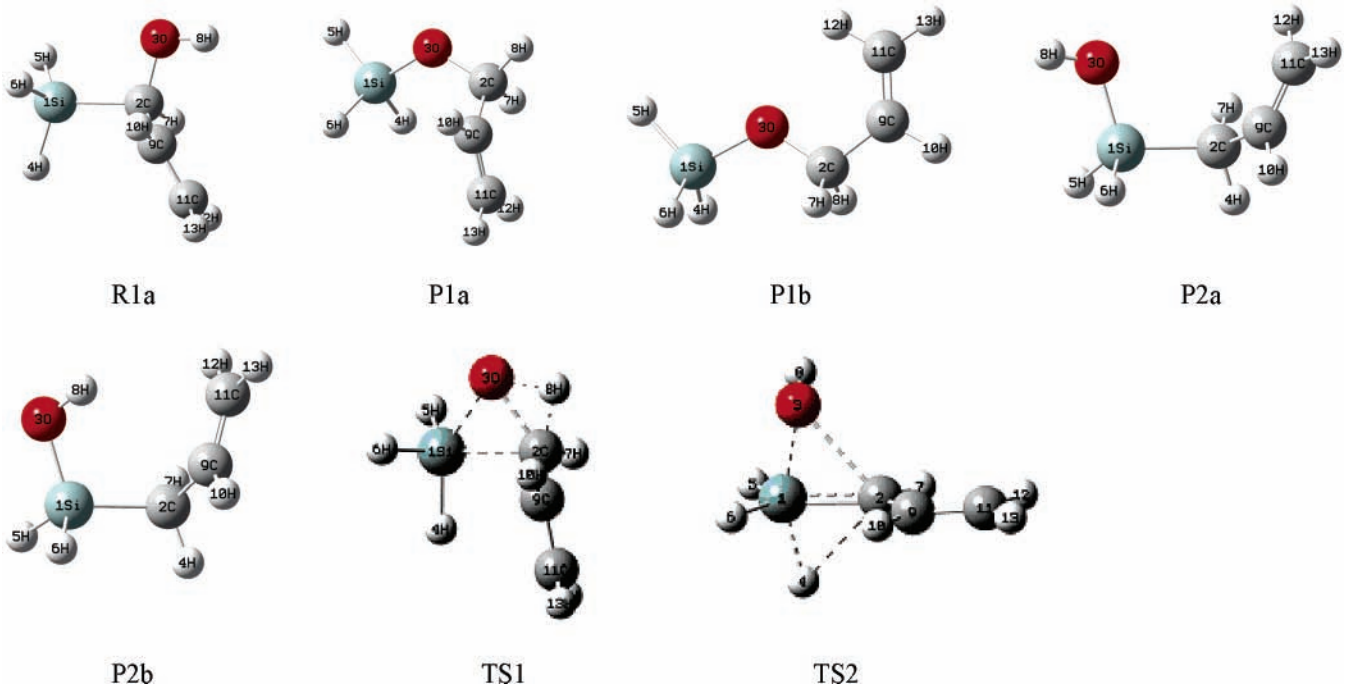

Figure 1. The MP2(full)/6-31G(d) geometries of stationary points.

TABLE 1: MP2(full)/6-31G(d) Structural Parameters[a]

parameter	R1a	P1a	P1b	P2a	P2b	TS1	TS2
Si−C^2	1.902	2.700	2.681	1.874	1.889	1.998	1.849
Si−O	2.667	1.672	1.668	1.672	1.670	1.865	1.801
C^2−O	1.441	1.434	1.425	2.836	2.888	1.646	2.282
Si−H^4	1.486	1.490	1.488			1.509	1.607
Si−H^5	1.484	1.480	1.478	1.491	1.481	1.485	1.498
Si−H^6	1.484	1.485	1.488	1.490	1.490	1.483	1.485
C^2−H^4				1.097	1.096		
C^2−H^7	1.103	1.099	1.101	1.096	1.096	1.088	1.096
C^2−H^8	1.961	1.094	1.101			1.236	
C^2−C^9	1.495	1.496	1.497	1.499	1.497	1.463	1.433
O−H^8	0.974			0.969	0.973	1.212	0.974
C^9−H^{10}	1.090	1.088	1.089	1.090	1.090	1.088	1.087
C^9−C^{11}	1.339	1.338	1.334	1.338	1.342	1.342	1.353
C^{11}−H^{12}	1.087	1.087	1.083	1.086	1.087	1.085	1.087
C^{11}−H^{13}	1.085	1.085	1.084	1.085	1.085	1.084	1.086
SiC^2O	104.9	32.3	32.7	34.5	33.3	60.6	50.4
H^4SiC^2	108.9	90.0	96.1	25.0	25.4	97.4	80.3
H^5SiC^2	110.3	131.6	133.7	110.4	112.1	115.9	124.3
H^6SiC^2	108.9	105.0	96.1	110.1	108.1	116.4	116.9
H^7C^2Si	109.2	91.8	91.6	108.1	108.8	101.6	118.6
H^8OSi	150.3	151.5	102.1	116.6	112.6	116.7	113.3
C^9C^2Si	111.3	95.5	110.4	111.4	108.1	108.1	127.2
$H^{10}C^9C^2$	115.4	116.1	115.1	116.2	116.5	116.6	118.5
$C^{11}C^9C^2$	124.4	123.3	124.3	124.8	124.8	122.7	121.3
H^4SiC^2O	173.9	139.1	125.5	165.4	−176.4	−178.3	176.8
H^5SiC^2O	53.8	21.5	0.0	120.6	117.4	72.7	89.5
H^6SiC^2O	−66.9	−112.0	−125.5	−120.7	−122.0	−69.6	−92.2
H^7C^2SiO	−118.8	−126.9	126.5	−49.3	−65.4	−110.7	−90.3
H^8OC^2Si	176.0	−174.9	−58.9	19.2	144.0	−169.7	−100.9
C^9C^2SiO	120.5	122.8	0.0	72.1	54.5	111.7	91.6
$H^{10}C^9C^2$Si	−67.7	−86.5	180.0	75.4	81.1	−92.0	0.3
$C^{11}C^9C^2$Si	111.3	92.6	0.0	−102.4	−94.7	89.0	−178.5
$H^{12}C^{11}C^9C^2$	1.5	0.4	0.0	−1.7	−5.3	−2.0	−1.0
$H^{13}C^{11}C^9C^2$	−177.9	180.0	180.0	178.1	177.4	175.7	178.5

[a] Bond lengths are in angstroms; bond and dihedral angles are in degrees.

TABLE 2: Total (a.u.) and Relative Energies (kJ/mol) of Stationary Points

struc-	MP2(full)/6−31(d)		G2(MP2)		G3	
ture	total	relative	total	relative	total	relative
R1a	−482.561463	0.0	−483.016153	0.0	−483.4996737	0.0
P1a	−482.603001	−109.1	−483.0522849	−94.9	−483.5365069	−96.7
P1b	−482.602363	−107.4	−483.0524347	−95.3	−483.5368015	−97.5
P2a	−482.628349	−175.6	−483.0835898	−177.1	−483.5695308	−183.4
P2b	−482.630617	−181.6	−483.0852559	−181.4	−483.5710895	−187.5
TS1	−482.427818	350.9	−482.8840448	346.8	−483.3688582	343.5
TS2	−482.466641	249.0	−482.9367471	208.5	−483.4220789	203.7

which groups on carbon and silicon atoms are staggered with respect to each other were proven not to be minimums at the MP2(full)/6-31G(d) levels. This is consistent with previous calculations.[18,31] First-order saddle points **TS1** and **TS2** were verified by IRC calculations (Figure 2) to be the transition states from **R1a** to **P1a** and from **R1a** to **P2a**, respectively. In **TS1** and **TS2**, silicon atoms are pentacoordinate. The distances of the Si−C^2, C^2−O, O−H,[8] Si−O, and C^2−H^8 bonds in **TS1** are 1.998, 1.865, 1.646, 1.236, and 1.212, respectively, which is a little longer than those in **R1a** and **P1a**, respectively, indicating that there are weak bonding interactions between Si and C^2, C^2 and O, O and H^8, Si and O, and C^2 and H^8. Therefore, **TS1** could be viewed as a bicyclic structure with two three-membered rings. In **TS2**, the atoms in the H^5H^6Si−C^2H^7−C^9H^{10}=$C^{11}H^{12}H^{13}$ moiety are nearly coplanar, and comparing the distances of Si−C^2 (1.849), C^2−C^9 (1.433), and C^9=C^{11} (1.353) with those in **R1a** (1.902, 1.495, and 1.339, respectively) and the atomic nature charges of Si, C^2, C^9, and C^{11} in **TS2** (1.326, −0.175, −0.381, and −0.194, respectively) with those

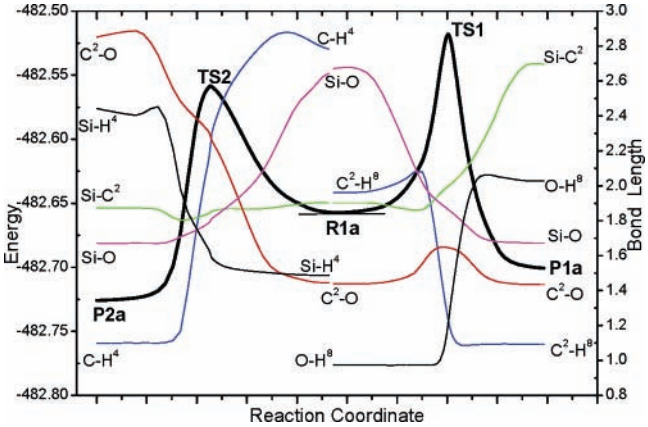

Figure 2. Energy and bond length vs reaction coordinate at the MP2(full)/6-31G(d) levels.

TABLE 3: Atomic Natural Charges

structure	Si	C^2	O	H^4	H^8	C^9	C^{11}
R1a	1.126	−0.321	−0.804	−0.230	0.484	−0.263	−0.412
P1a	1.409	−0.051	−0.980	−0.266	0.218	−0.259	−0.405
P1b	1.418	−0.050	−0.981	−0.265	0.196	−0.249	−0.408
P2a	1.676	−0.976	−1.144	0.245	0.510	−0.209	−0.428
P2b	1.672	−0.978	−1.149	0.250	0.514	−0.203	−0.465
TS1	1.367	−0.646	−0.807	−0.290	0.554	−0.241	−0.436
TS2	1.326	−0.175	−1.145	−0.341	0.480	−0.381	−0.194

TABLE 4: Activation Energies of Thermal Rearrangements of 1-Silylprop-2-en-1-ol and Silylmethanol at the G2(MP2) Level

reactions	1-silylprop-2-en-1-ol	silylmethanol[18]
A	346.8	348.2
B	208.5	240.9

in **R1a** (1.126, −0.321, −0.263, and, −0.412, respectively) and **P2a** (1.676, −0.976, −0.209, and −0.428, respectively), both the bond lengths of Si−C^2-C^9=C^{11} and the atomic nature charges of Si, C^2, C^9, and C^{11} are averaged to some extent. This suggests that there exists a four-centered π bond in Si−C^2−C^9=C^{11} and the valence electrons in the H^5H^6Si−C^2H^7−C^9H^{10}=$C^{11}H^{12}H^{13}$ moiety of **TS2** are delocalized. Similarly to **TS1**, **TS2** can also be viewed as a bicyclic structure with two three-membered rings.

3.2. [1, 2] Thermal Rearrangement of Silyl group from Carbon to Oxygen. The IRC calculations (see Figure 2) show that the [1, 2] thermal rearrangement of the silyl group (H_3Si−) of $H_3SiCH(OH)CH$=CH_2 from carbon to oxygen atom to form allyloxysilane happens as a one-step transposition passing through transition state **TS1** (Scheme 3, path A). The reaction begins as the oxygen atom of **R1a** moves toward the silicon atom. At the beginning, the C^2−O bond weakens, the Si−C^2 bond length shortens, and the C^2−H^8 distance lengthens, but the O−H^8 bond length has hardly changed. As the oxygen atom further approaches the silicon atom, the Si−C^2 bond length reaches a minimum and then begins to lengthen, and the H^8 begins to leave the oxygen atom and move toward the C^2 rapidly. Before the O−H^8 bond fully dissociates, the C^2−O distance reaches its maximum and then begins to shorten. As a result, the transition state, **TS1**, is reached. The C^2−O and O−H^8 distances increase from 1.441 and 0.974 in **R1a** to 1.646 and 1.212 in **TS1**, respectively. Meanwhile, the Si−O and C^2−H^8 distances reduce from 2.667 and 1.966 to 1.961 and 1.236, respectively. The activation barrier for reaction A is 343.5 kJ/mol at the G3 level.

After getting over the transition state, the H^8 gradually bonds to the C^2 as the oxygen atom further approaches the silicon

TABLE 5: Vibrational Frequencies[a] (cm^{-1}) of R, TS1,TS2, P1a, and P2a

R1a	3516(22), 3115(10), 3031(2), 3021(8), 2865(29), 2197(160), 2190(145), 2176(86), 1620(3), 1411(5), 1312(14), 1269(2), 1241(11), 1164(17), 1092(12), 1013(46), 978(41), 931(61), 925(45), 914(125), 885(26), 872(185), 766(37), 655(32), 587(29), 551(22), 446(16), 339(123), 300(3), 242(5), 205(4), 138(2), 79(1)
P1a	3117(10), 3042(4), 3026(6), 2972(25), 2899(37), 2214(174), 2183(149), 2164(140), 1631(2), 1480(3), 1416(12), 1341(9), 1266(0.5), 1239(7), 1145(16), 1067(156), 982(11), 958(30), 926(131), 971(436), 952(89), 901(36), 900(3), 743(23), 719(56), 695(57), 620(14), 413(0.7), 337(5), 219(3), 149.6(1), 95(1), 71(2)
P2a	3618(88), 3117(13), 3032(3), 3018(15), 2974(4), 2917(9), 2155(171), 2151(256), 1630(11), 1424(10), 1400(7), 1282(1), 1189(37), 1181(7), 1032(54), 975(74), 972(62), 951(241), 916(11), 862(40), 828(155), 815(58), 760(14), 715(64), 692(103), 578(17), 553(25), 388(3), 242(5), 198(2), 163(125), 70(3), 55(2)
TS1	−1747(866), 3131(6), 3044(3), 3043(2), 3035(4), 2331(101), 2188(182), 2165(124), 2037(239), 1605(8), 1405(8), 1269(2), 1205(45), 1134(12), 1033(142), 1016(101), 959(160), 956(49), 932(8), 870(309), 839(26), 766(56), 710(75), 701(3), 655(72), 558(114), 516(130), 443(17), 375(33), 260(6), 166(2), 120(2), 77(2)
TS2	−623(229), 3553(70), 3122(3), 3061(2), 3028(2), 2981(6), 2165(157), 2092(190), 1629(247), 1584(84), 1422(80), 1281(1), 1223(12), 1176(57), 1034(74), 998(22), 984(111), 967(4), 962(41), 892(39), 857(121), 829(236), 712(37), 628(15), 599(16), 592(143), 490(131), 398(102), 346(43), 265(9), 168(10), 154(3), 84(0.3)

[a] IR intensity (km/mol) in parentheses.

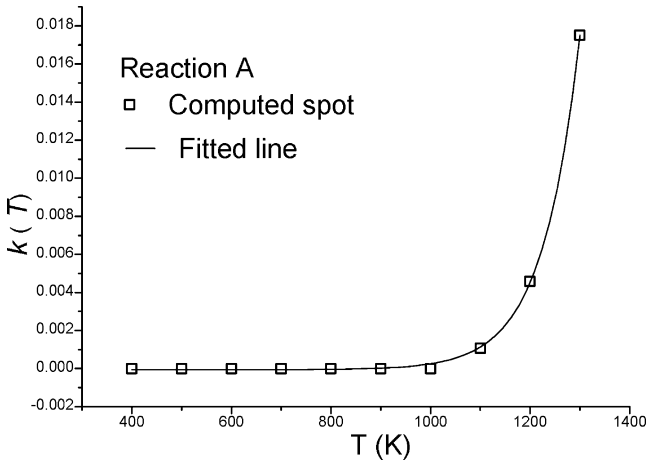

Figure 3. $k(T)$ against temperature T for reaction **A**.

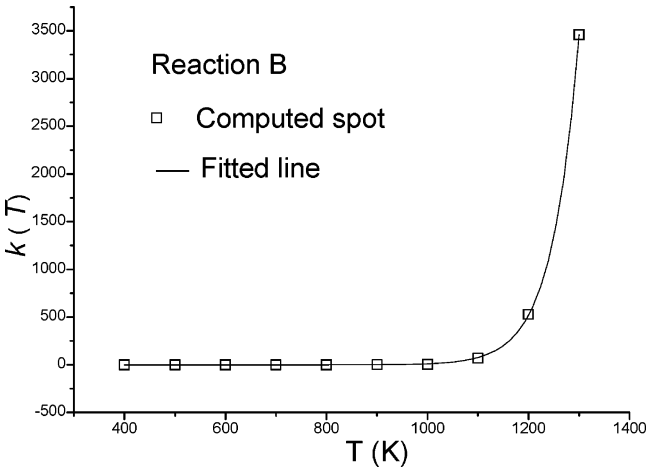

Figure 4. $k(T)$ against temperature T for reaction **B**.

atom, and the C^2 leaves the silicon atom and approaches the oxygen atom continuously, coupled with the rotation of the $-C^2H_2C^9$ group around an axis perpendicular to the $SiOC^2$ plane in the direction of H^8 apart from the oxygen atom. As a result, the product, **P1a**, forms as the oxygen atom fully bonds to the C^2 and the $Si-C^2$ bond fully dissociates. The IRC calculations show that during the [1, 2] migration of the silyl group, its configuration is sterically retained.

The rearrangement reaction, **A**, can also be analyzed from the change of the MP2(full)/6-31G(d) atomic natural charges on the basis of the MP2(full)/6-31G(d) optimized geometries as shown in Table 3. As the reaction proceeds, the partial lone pair of electrons on the oxygen atom transfer to the silicon atom, more valence electrons of the silicon atom transfer to C^2, and the partial valence electrons of C^2 transfer to the oxygen atom, leading to the corresponding increases of positive charge on the silicon atom and negative charge on the C^2 and the oxygen atom in **TS1**. When **P1a** forms, the $Si-C^2$ bond cleaves and the silicon atom bonds to the oxygen atom, with the result that more valence electrons of the silicon atom transfer to the oxygen atom, resulting in an increasing of positive charge on the silicon atom by 0.042 and negative charge on the oxygen atom by 0.173 and a decrease in the negative charge on the C^2 by 0.595 in **P1a**, in comparison with **TS1**.

3.3. Thermal Dyotropic Rearrangement Reaction. The IRC calculations indicate that the thermal dyotropic rearrangement (Scheme 3, path B) of the hydroxyl group of $H_3SiCH(OH)-CH=CH_2$ from carbon atom to silicon atom coupled with a simultaneous migration of a hydrogen atom from silicon atom to carbon atom, to form allylsilanol **P2,** is a one-step transformation passing through transition state **TS2** in which the silicon is pentacoordinate. The reaction begins as the hydroxyl group of reactant **R1a** moves toward the silicon, coupled with the inverse motion of H^7 and C.[9] It can be seen from Figure 2 that, at the beginning of the reaction, the C^2-O and $Si-H^4$distances lengthen slowly. As the hydroxyl group further approaches the silicon atom, the distances of the C^2-O and $Si-H^4$ lengthen rapidly, and the transition state, **TS2**, is reached. The Si−O distance reduces from 2.667 in **R1a** to 1.801 in **TS2**, and the C^2-O and $Si-H^4$ distances increase from 1.441 and 1.486 to 2.282 and 1.607, respectively. With the interaction of the lone pair of electrons on the oxygen atom and the empty 3d orbital of the silicon atom in **TS2**, the valence electrons of the silicon atom partially transfer to the oxygen atom, resulting in an increase in the positive charge on the silicon atom and the negative charge on the oxygen atom and a decrease in the negative charge on the C^2 atom (see Table 3). The G3 activation barrier for the reaction is 203.7 kJ/mol, lower by 139.8 kJ/mol than rearrangement **A**.

After getting over the transition structure, the hydroxyl group continuously approaches the silicon atom and H^4 departs from the silicon atom and moves toward the C^2 atom. As a result, the hydroxyl group bonds to the silicon atom, coupled with the full dissociation of the $Si-H^4$ bond and the formation of the C^2-H^4 bond, and product **P2a** forms.

In comparison with the relative rearrangement of silylmethanol H_3SiCH_2OH,[18] the G2(MP2) activation energy of reaction **A** of $H_3SiCH(OH)CH=CH_2$ is only 1.4 kJ/mol lower, whereas for reaction **B**, the activation energy of $H_3SiCH(OH)CH=CH_2$ is 32.4 kJ/mol lower (see Table 4). This suggests that substitu-

tion of the vinyl group on the center carbon atom, forming an allylic structure, is in favor of reaction **B** because of the effect of the Si—C^2—C^9═C^{11} four-centered π bond in **TS2** as discussed already, which makes **TS2** more stable than the corresponding transition state of the rearrangement of silylmethanol and then lowers the activation energy of reaction **B** of $H_3SiCH(OH)$-$CH{=}CH_2$.

3.4. Thermodynamic and Kinetic Analyses. Thermodynamic and kinetic analyses can further illustrate the realizability and possibility of a reaction. There are many reports on theoretical research of thermodynamic and kinetic properties.[24−27,32,33] We carried out the thermodynamic and kinetic calculations for rearrangements **A** and **B** on the basis of the MP2(full)/6-31G(d) optimized parameters, zero-point corrected energies, scaled (by 0.9427) vibrational frequencies (see Table 5), and Hessian matrix (see Supporting Information) in statistical mechanical methods and canonical variational transition-state theory (CVT) with small-curvature tunneling approximation (SCT) over a temperature range from 400 to 1300 K.

To calculate the rate constants, 30 points were selected for each reaction near the transition state along the minimum-energy path calculated by the IRC definition, with 15 points respectively in the reactant and product sides. For the purpose of comparison, TST rate constants were also calculated. The calculated thermodynamic changes, equilibrium constants, and rate constants are listed in Table 6.

The following points can be found from the data in Table 6: (1) For the two reactions, the differences of the TST and CVT rate constants are remarkable, indicating that variational effects on the two reactions are large. (2) The ΔH and ΔG values for the two reactions are all negative, indicating that they are exothermic and spontaneous. As the temperature rises, the exothermicity and the ΔG values of reaction **A** increase. For reaction **B**, the exothermicity increases slightly over the whole studied temperature range, whereas the ΔG value decreases gradually. (3) The equilibrium constant $K(T)$ and the CVT and TST rate constant $k(T)$ of reaction **B** are larger than those of reaction **A** at the same temperature. This suggests that the rearrangements of **R** are favorable to route **B** both thermodynamically and kinetically. So, when **R** is heated to a certain temperature, the main rearrangement product would be **P2**.

Figures 3 and 4 show the CVT/SCT rate constants against temperature for reactions **A** and **B,** respectively, over a temperature range from 400 to 1300 K. The relationship between rate constant $k(T)$ and temperature T conforms to the following equations:

$$k(T)_{\mathbf{A}} = -6.0 \times 10^{-5} + 4.35 \times 10^{-10}\, e^{0.01347T}$$

$$k(T)_{\mathbf{B}} = -2.39 + 6.92 \times 10^{-8}\, e^{0.01895T}$$

4. Conclusions

The calculations show that two rearrangement reactions may occur when 1-silylprop-2-en-1-ol is heated. One is via the Brook rearrangement reaction, in which the silyl group migrates from the carbon to the oxygen atom passing through a double three-membered-ring transition state, forming allyloxysilane; the other is a dyotropic rearrangement, in which the hydroxyl group of **R** migrates from carbon atom to silicon atom coupled with a simultaneous migration of a hydrogen atom from silicon atom to carbon atom, via a double three-membered-ring transition state, forming allylsilanol. Silicon atoms in the two transition states are pentacoordinate. The barrier for the Brook rearrangement was computed to be 343.5 kJ/mol at the G3 level, 139.8 kJ/mol higher than that for the dyotropic rearrangement reaction (203.7 kJ/mol). Thermodynamic and kinetic analyses indicate that the dyotropic rearrangement reaction is preferred to the Brook rearrangement reaction, both thermodynamically and kinetically. When compared with the relevant rearrangements of silylmethanol H_3SiCH_2OH, for reaction **B**, the activation energy of rearrangement of $H_3SiCH(OH)CH{=}CH_2$ is 32.4 kJ/mol lower at the G2(MP2) level. This should be attributed to the substitution of the vinyl group on the center carbon atom, which forms an allylic structure and leads to the Si—C^2—C^9═C^{11} four-centered π bond in the transition state **TS2,** thus making **TS2** more stable than the corresponding transition state of the rearrangement of silylmethanol in which the electron delocalization effect does not exist, and lowers the activation energy of reaction **B** of $H_3SiCH(OH)CH{=}CH_2$, whereas the substitution of the vinyl group has almost no effect on the activation energy of reaction **A**.

TABLE 6: Thermodynamic and Kinetic Analyses

T (K)	$\Delta S^{\ddagger}$ (J/K)	ΔS (J/K)	ΔH (kJ/mol)	ΔG (kJ/mol)	$k_{CVT/SCT}$ (s^{-1})	$k_{TST/SCT}$ (s^{-1})	K (T)
				Reaction **A**			
400	−2.81	−2.44	−105.9	−105.0	1.97×10^{-30}	1.47×10^{-29}	4.55×10^{13}
500	−3.12	−4.01	−106.6	−104.6	8.94×10^{-23}	7.59×10^{-22}	7.81×10^{10}
600	−3.47	−5.09	−107.2	−104.2	2.64×10^{-17}	2.46×10^{-16}	1.09×10^{9}
700	−3.83	−5.83	−107.7	−103.6	2.67×10^{-13}	2.67×10^{-12}	5.06×10^{7}
800	−4.19	−6.34	−108.1	−103.0	2.93×10^{-10}	3.09×10^{-9}	5.02×10^{6}
900	−4.55	−6.69	−108.4	−102.4	7.08×10^{-8}	7.81×10^{-7}	8.26×10^{5}
1000	−4.91	−6.94	−108.6	−101.7	5.86×10^{-6}	6.68×10^{-5}	1.94×10^{5}
1100	−5.26	−7.11	−108.8	−101.0	7.41×10^{-4}	8.39×10^{-3}	5.88×10^{4}
1200	−5.62	−7.23	−108.9	−100.3	4.59×10^{-3}	5.50×10^{-2}	2.20×10^{4}
1300	−5.96	−7.32	−109.0	−99.5	1.75×10^{-2}	7.36×10^{-1}	9.50×10^{3}
				Reaction **B**			
400	−3.14	10.53	−170.4	−174.6	7.71×10^{-19}	8.60×10^{-19}	5.41×10^{22}
500	−3.39	10.47	−170.4	−175.7	1.15×10^{-12}	1.31×10^{-12}	1.96×10^{18}
600	−3.69	10.36	−170.5	−176.7	1.64×10^{-8}	1.88×10^{-8}	2.14×10^{15}
700	−4.05	10.22	−170.6	−177.7	1.57×10^{-5}	1.83×10^{-5}	1.64×10^{13}
800	−4.45	10.04	−170.7	−178.7	2.78×10^{-3}	3.28×10^{-3}	4.22×10^{11}
900	−4.88	9.87	−170.9	−179.7	1.58×10^{-1}	1.88×10^{-1}	2.45×10^{10}
1000	−5.32	9.69	−171.0	−180.7	4.02×10^{0}	4.84×10^{0}	2.51×10^{9}
1100	−5.78	9.52	−171.2	−181.6	6.72×10^{1}	8.09×10^{0}	1.30×10^{8}
1200	−6.23	9.37	−171.4	−182.6	5.28×10^{2}	6.45×10^{2}	8.18×10^{7}
1300	−6.68	9.23	−171.6	−183.5	3.46×10^{3}	4.26×10^{3}	2.19×10^{7}

Acknowledgment. The authors thank Professor Donald G. Turhlar for providing the *POLYRATE 9.0* program and Professor Qingzhu Zhang, Doctor Jun Zhang of Shandong University, and Yan Zhao of Minnesota University for their help in using *POLYRATE*. This work was supported by the National Natural Science Foundation of China, the Natural Science Foundation of Shandong Province, Reward Funds for the Outstanding Young by Shandong University, Foundation for University Key Teacher by the Ministry of Education, and Scientific Research Starting Fundation for the Return Overseas Chinese Scholar by the Ministry of Education.

Supporting Information Available: Data needed for CVT rate constant calculations. This material is available free of charge via the Internet at http://www.pubs.acs.org.

References and Notes

(1) Du, Z. D.; Chen, J. H.; Bei, X. L.; Zhou, C. G. *Organosilicon Chemistry*; The High Education Press: Beijing, 1992; pp 175−177.
(2) Brook, A. G. *Acc. Chem. Res*. **1974**, *7*, 77−84.
(3) Reich, H. J.; Holtan, R. C.; Bolm, C. *J. Am. Chem. Soc*. **1990**, *112*, 5609−5617.
(4) Dalton, J. C.; Bourque, R. A. *J. Am. Chem. Soc*. **1981**, *103*, 699−700.
(5) Tsai, Y.-M.; Cherng, C.-D. *Tetrahedron Lett*. **1991**, *32*, 3515−3518.
(6) Chang, S.-Y.; Jiaang, W.-T.; Cherng, C.-D.; Tang, K.; Hang, C.-H.; Tsai, Y.-M. *J. Org. Chem*. **1997**, *62*, 9089−9098.
(7) Robertson, J.; Burrow, J. N. *Tetrahedron Lett*. **1994**, *35*, 3777−3780.
(8) Paredes, M. D.; Alonso, R. *Tetrahedron Lett*. **1999**, *40*, 3973−3976.
(9) Paredes, M. D.; Alonso, R. *J. Org. Chem*. **2000**, *65*, 2292−2304.
(10) Harris, J. M.; MacInnes, I.; Dalton, J. C.; Maillard, B. *J. Organomet. Chem*. **1991**, *403*, C25−C28.
(11) Wright, A.; West, R. *J. Am. Chem. Soc*. **1974**, *96*, 3214−3222.
(12) Linderman, R. J.; Ghannam, A. *J. Am. Chem. Soc*. **1990**, *112*, 2392−2398
(13) Shuto, S.; Kanazaki, M.; Ichikawa, S.; Minakawa, N.; Matsuda, A. *J. Org. Chem*. **1998**, *63*, 746−754.
(14) Antoniotti, P.; Tonachini, G. *J. Org. Chem*. **1993**, *58*, 3622−3632.
(15) Antoniotti, P.; Canepa, C.; Tonachini, G. *J. Org. Chem*. **1994**, *59*, 3952−3959.
(16) Wang, Y.-G.; Dolg, M. *Tetrahedron* **1999**, *55*, 12751−12756.
(17) Schiesser, C. H.; Styles, M. L. *J. Chem. Soc., Perkin Trans. 2* **1997**, *2*, 2335−2340.
(18) Yu, Y.; Feng, S. *J. Phys. Chem. A* **2004**, *108*, 7468−7472.
(19) Reetz, M. T. *Angew. Chem., Inter. Ed. Eng*. **1972**, *11*, 129−131.
(20) Foresman, J. B.; Frisch, A. *Exploring Chemistry with Electronic Structure Methods*, 2nd ed.; Gaussian, Inc.: Pittsburgh, PA, 1996; p 64.
(21) Curtiss, L. A.; Krishnan, R.; Pople, J. A. *J. Chem. Phys*. **1993**, *98*, 1293.
(22) Curtiss, L. A.; Raghavachari, K.; Redfern, P. C.; Rassolov, V.; Pople, J. A. *J. Chem. Phys*. **1998**, *109*, 7764.
(23) Frisch, M. J.; Trucks, G. W.; Schlegel, H. B.; Scuseria, G. E.; Robb, M. A.; Cheeseman, J. R.; Zakrzewski, V. G.; Montgomery, J. A., Jr.; Stratmann, R. E.; Burant, J. C.; Dapprich, S.; Millam, J. M.; Daniels, A. D.; Kudin, K. N.; Strain, M. C.; Farkas, O.; Tomasi, J.; Barone, V.; Cossi, M.; Cammi, R.; Mennucci, B.; Pomelli, C.; Adamo, C.; Clifford, S.; Ochterski, J.; Petersson, G. A.; Ayala, P. Y.; Cui, Q.; Morokuma, K.; Malick, D. K.; Rabuck, A. D.; Raghavachari, K.; Foresman, J. B.; Cioslowski, J.; Ortiz, J. V.; Stefanov, B. B.; Liu, G.; Liashenko, A.; Piskorz, P.; Komaromi, I.; Gomperts, R.; Martin, R. L.; Fox, D. J.; Keith, T.; Al-Laham, M. A.; Peng, C. Y.; Nanayakkara, A.; Gonzalez, C.; Challacombe, M.; Gill, P. M. W.; Johnson, B. G.; Chen, W.; Wong, M. W.; Andres, J. L.; Head-Gordon, M.; Replogle, E. S.; Pople, J. A. *Gaussian 98*, revision A.9; Gaussian, Inc.: Pittsburgh, PA, 1998.
(24) Ju, G.; Feng, D.; Deng, C. *Acta Chim. Sin*. **1985**, *43*, 680.
(25) Baldrige, K. K.; Gordor, M. S.; Steckler, R.; Truhlar, D. G. *J. Phys. Chem*. **1989**, *93*, 5107.
(26) Gonzalez-Lafont, A.; Truong, T. N.; Truhlar, D. G. *J. Chem. Phys*. **1991**, *95*, 8875.
(27) Garrett B. C.; Truhlar, D. G. *J. Phys. Chem*. **1979**, *83*, 1052.
(28) Chuang, Y.-Y.; Truhlar, D. G. *J. Chem. Phys*. **2000**, *112*, 1221−1228.
(29) Liu, Y.-P.; Lynch, G. C.; Truong, T. N.; Lu, D.-H.; Truhlar, D. G.; Garrett, B. C. *J. Am. Chem. Soc*. **1993**, *115*, 2408.
(30) Steckler, R.; Chuang, Y. Y.; Fast, P. L.; Corchade, J. C.; Coitino, E. L.; Hu, W. P.; Lynch, G. C.; Nguyen, K.; Jackells, C. F.; Gu, M. Z.; Rossi, I.; Clayton, S.; Melissas, V.; Garrett, B. C.; Isaacson, A. D.; Truhlar, D. G. *POLYRATE*, version 9.0; University of Minnesota: Minneapolis, MN, 2002.
(31) (a) Ignat'ev, I. S.; Shchegolev, B. F. *Dokl. Akad. Nauk SSSR* **1987**, *296* (1), 143−147. (b) Grigoras, S.; Lane, T. H. *J. Comput. Chem*. **1987**, *8*, 84. (c) Oberhammer, H.; Boggs, J. E. *J. Am. Chem. Soc*. **1980**, *102*, 7241. (d) Raghavachari, K.; Chandrasekhar, J.; Frisch, M. J. *J. Am. Chem. Soc*. **1982**, *104*, 3779.
(32) (a) Sumathi, R.; Green, W. H., Jr. *Theor. Chim. Acta* **2002**, *108*, 187−213. (b) Sumathi, R.; Green, W. H., Jr. *J. Phys. Chem. A* **2001**, *105*, 6910−6925. (c) Sumathi, R.; Green, W. H., Jr. *Phys. Chem. Chem, Phys.* **2003**, *5*, 3402−3417.
(33) Van Speybroeck, V.; Van Neek, D.; Waroquier, M. *J. Phys. Chem. A* **2000**, *104*, 10939−10950.